Journal of GeoEngineering, Vol. 14, No. 3, pp. 191-202, September 2019
http://dx.doi.org/10.6310/jog.201909_14(3).7

Case Study

EVALUATION OF THE TRUNCATED SOLDIER PILE BEHAVIOR IN AN ANCHORED DEEP EXCAVATION CASE STUDY BY THE AID OF 3D AND 2D FINITE ELEMENT ANALYSES

Javad Jalili [1*] and Mojtaba Moosavi [2]

ABSTRACT

In recent years many deep excavations are being conducted in urban areas of Iran, where anchored soldier piles (Berlin method) are commonly preferred as the retaining structure of the excavations. However, in some cases due to economical purposes, the soldier pile is not continued down to beneath the bottom of the excavation but is truncated somewhere between the excavation top and bottom. Such a shortened pile is called a Truncated Soldier (TS) pile in this study. Although a TS pile is believed to strengthen the local area covered by its length, it cannot provide vertical support for the retaining structure. This dominant disadvantage of the TS pile may lead to excessive settlements around the excavation. As a related case study, this paper describes the process of innovative 3D and 2D calculations utilized to improve the construction process of a 26.5 m deep excavation. The Initial excavation design contained many TS piles. Consequently, when the digging reached the depth of 18 to 24 meters, disturbing cracks showed up in some neighboring streets and structures. The excavation was stopped and a recalculation and optimization of the initial design and construction stages was done. The optimization guidelines were extracted from innovative numerical simulations. Following the guidelines, the remainder of the excavation was cleared successfully under precise monitoring. The reasonable agreement of the numerical results with those of the instrumentation at the site proved the applicability of the suggested 3D and 2D calculations in the excavation design. It is also shown that the TS piles are not reliable for deep excavations.

Key words: Deep excavation, soldier pile, anchored shotcrete wall, 3D numerical analysis, 2D numerical analysis.

1. INTRODUCTION

The development of urban living in big cities has led to deep diggings in the ground to achieve the most possible space for the human living needs. Although detailed regulations exist regarding excavation design and construction processes (Sabatini *et al.* 1999), the required investigations and calculations are not always provided sufficiently due to the complicated soil behavior and also economic interests.

In recent years many deep excavations have been conducted in populated cities of Iran. The anchored soldier pile (the Berlin method, Puller 2003) is popular among Iranian engineers. However, a recently growing practice is to truncate the soldier piles before reaching the bottom of the excavation. In such cases the vertical support of the retaining structure relies on the friction of the shotcrete walls with the adjacent soil. The Truncated Soldier (TS) piles behave as a local stiffener for the limited area behind them. Although the shortened pile is economically interesting, there is no guaranty that sufficient vertical support is provided by the soil-shotcrete friction. Even if the vertical support is provided, the consequent settlement may be considerable. This paper is trying to show these shortcomings of TS piles by investigating a real case study.

In this paper a 26.5 m deep excavation design and construction procedure is reviewed as the case study. The excavation was carried out in a crowded area of a big city in Iran. Due to the incompetent performance of the numerous TS piles embedded throughout the excavation wall, excessive settlements stopped the project before reaching the intended depth. The retaining structure was strengthened through design improvements based on numerous innovative 3D and 2D numerical models, as will be stated through the paper. The excavation was continued with regard to the improved design and construction guidelines. The guidelines included detailed monitoring by several inclinometers located all over the excavation walls. The successful completion of the excavation with satisfactory matching monitored and calculated settlements, proved the proposed guidelines effective to be followed in similar cases.

2. CASE STUDY DESCRIPTION

2.1 Site Condition

To construct a tall building in a populated city of Iran, a 26.5 m deep excavation was required. The site-plan of the excavation was a vast area of 6.5 hectares with numerous neighboring buildings. A detailed geotechnical investigation was carried out which included 33 boreholes of 30 to 90 m depth (JahadAzma 2015). Figure 1 shows the excavation site-plan and the borehole

Manuscript received November 27, 2018; revised April 22, 2019; accepted May 20, 2019.
[1*] Assistant Professor (corresponding author), Geotechnical research center, International Institute of Earthquake Engineering and Seismology, Tehran, 19395/3913, Iran (e-mail: suraparb@hotmail.com).
[2] Assistant Professor, Geotechnical research center, International Institute of Earthquake Engineering and Seismology, Tehran, 19395/3913, Iran.

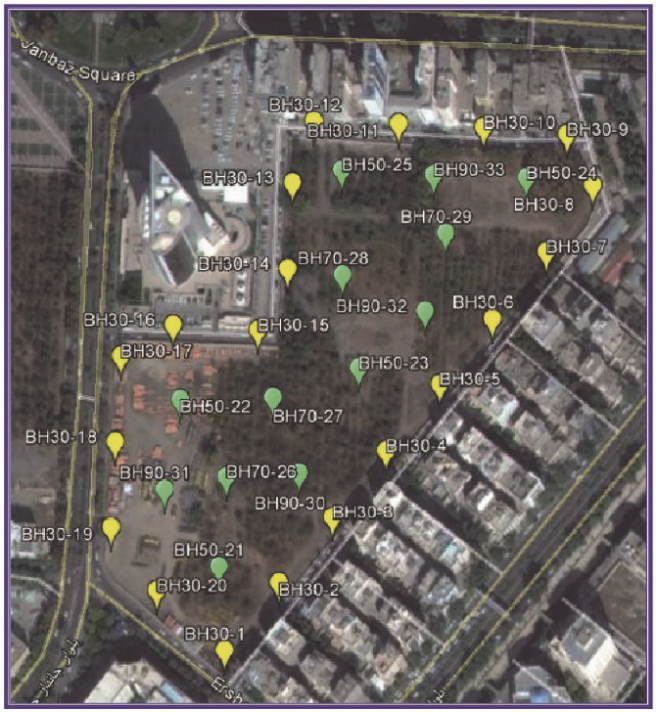

Fig. 1 Site plan of the excavation and the borehole locations

locations. Plenty in-site and laboratory experiments were conducted at different levels of the boreholes and on numerous soil samples. This data was helpful in preference of soil properties for complementary analyses conducted in this study.

The Standard Penetration Test (SPT) results showed that the soil layers mainly contain medium-dense to dense cohesionless soils, including limited low-plastic cohesive layers at depths 20 m to 30 m. The shear strength parameters were preferred by weighted averaging among triaxial CU tests, slow direct shear tests, pressuremeter tests, and SPT data. The soil deformation parameters both in loading and unloading were also preferred by engineering judgement among above mentioned data, getting closer to values obtained from pressuremeter and SPT tests in coarse grained soils. Table 1 shows the final proposed soil layering and soil properties. The water table depth was reported 40 m, which was well below the final depth of excavation.

The initial design included several TS piles in different sections of the widely extended excavation walls with a total perimeter of 1200 m. Figure 2(a) shows the general view of the excavation area and Fig. 2(b) shows the installed TS piles.

TS piles consisted of two IPE200 steel profiles, 6 m long with 3 m spacing, which were installed before excavation initiation. After installing the TS pile in the bored shaft, an easily crushable lean concrete was used to fill the voids of the shafts. The length of the anchors was 26 m at top elevations, reducing gradually to 18 m at the bottom of the excavation wall, with 10 to 15 degrees of inclination from horizontal direction. The anchors were pre-stressed up to 800 kN after installation and relied on concrete pads designed to tolerate the pre-stress force. The shotcrete walls with 5 ~ 10 cm thickness included wire mesh of ϕ6 @15 mm with 25 MPa strength.

2.2 Spreading of Cracks

When the excavation reached 24 m of depth, cracks started to spread considerably in the vicinity of the site, as shown in Fig. 3.

Table 1 Soil layering and properties at the site (JahadAzma 2015)

Layer depth (m)	C_s	C_c	P_c (kPa)	ν	E_r (kPa)	E (kPa)	ϕ′ (°)	c' (kPa)	E_p (kPa)	E_s (kPa)	E_s (kPa)	ϕ′ (°)	ϕ′ (°)	c' (kPa)	ϕ′ (°)	Corrected SPT N values range	Moisture (%)	Unit weight (kN/m^3)	Layer thickness (m)	Soil classification
	Final Selection								PMT	Triaxial	SPT	SPT	Laboratory Results		PMT*	N_c				
0 ~ 9	–	–	–	0.3	–	2E4	28	15	25300	14200	10800	–	28	14	–	28~38	18.5	16.1	9	CL-ML, CL
9 ~ 30	–	–	–	0.25	16E4	4E4	35	10	60400	24100	28700	34	31	10	42	23~32	6	19	21	SM, SC-SM
30 ~ 44	0.026	0.220	200	0.3	11E4	24E3	28	12	34200	10200	8500	–	28	12	–	23~26	22	16	14	CL, CL-ML
44 ~ 90	0.026	0.220	250	0.5	14E4	3E4	27	14	52400	13500	7900	–	27	14	–	13~26	26	15.8	46	CL, ML

* Pressure meter test

(a) General view

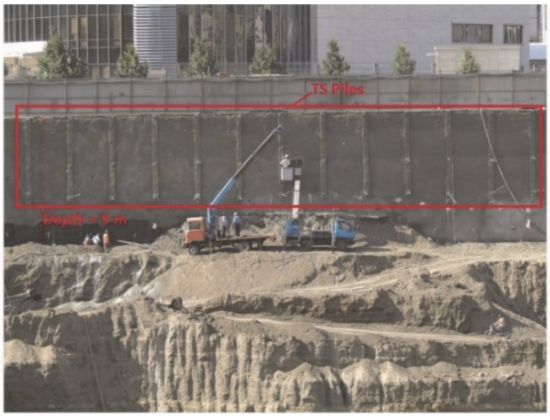

(b) Truncated soldier piles

Fig. 2 Case study: A 26.5 m deep excavation

Fig. 3 Propagated cracks in the vicinity of the site after 24 m of excavation

Unfortunately, the excavation was not instrumented to be monitored from the beginning, nor was the initial design reliable to assure a safe further excavation. Therefore, the project was stopped to improve the excavation design and practice. A more precise calculation and design was required to guarantee a safe guideline for the remainder of the excavation.

3. IMPROVEMENT OF THE EXCAVATION DESIGN AND CONSTRUCTION

3.1 3D Calculations

The initial excavation design was examined by the aid of PLAXIS 3D 2016 (PLAXIS 3D 2016) code. A 3D modeling was necessary to simulate the excavation stages carried out at the site, such as excavating alternate 15 m spans, as shown in Fig. 4. As depicted in this figure, each 15 m excavated span was bordered by two adjacent un-excavated spans. This alternate-span excavation technique decreased the probable deformations caused by the soil removal. To simulate the initial design more precisely, the method of excavation could not be ignored in the numerical simulations. Further analyses showed the importance of such detailed numerical modeling, as will be stated in the paper.

Hardening Soil (HS) model was preferred as the constitutive model of the numerical simulation. The HS model is based on the hyperbolic model and also benefits from isotropic hardening both in shearing and compression loadings (Schanz *et al.* 1999). The model calibration was based on extensive soil experiments which were conducted during the site investigations. Table 2 shows the calibrated parameters of the model. The slight differences of the parameters magnitudes with those of Table 1 is due to the difference of engineering judgment of the geotechnical surveying engineers (JahadAzma Co. 2015) which lead to the table 1 magnitudes, and the judgement of the authors of this paper which lead to those of Table 2.

One of the advantages of PLAXIS code is providing proper tools for modeling structural elements in an excavation simulation:

The soldier piles were modeled by “embedded pile” element of the code, composed of beam elements and especial interface elements capable of interacting with subsoil. Ground anchors were modelled using “node-to-node anchor” element, connected to “embedded pile” element. While the latter would be the grouted part of the anchor capable of having skin and foot resistance, the former is like a spring connecting two points, resembling the ungrouted part of the anchor. Combination of beam and plates were also utilized to model surrounding buildings and structures. The shotcrete was modeled by plate elements with 15 cm thickness and linear elastic behavior with elastic modulus of 10^6 kPa.

The material model of the soldier piles and the grouted piles of the anchor (embedded pile) was preferred to be linear elastic, and the ungrouted part of the anchor (node-to-node anchor) was modeled elastoplastic, with defined maximum compression and tension capacity. Tables 3 and 4 include parameters of the structural elements applied in the numerical analysis. Detailed information on the above mentioned elements could be found in PLAXIS manual (Brinkgreve *et al.* 2016).

Fig. 4 Alternate-span excavation of 15 m length and 2 m thickness

Table 2 Calibrated parameters of Hardening-Soil material model applied in numerical analysis

Parameter	Symbol	Unit	Layer 1 (0 ~ 2 m)	Layer 2 (2 ~ 9 m)	Layer 3 (9 ~ 30 m)	Layer 4 (30 ~ 44 m)	Layer 5 (44 ~ 70 m)
Dry unit weight	γ_{unsat}	kN/m^3	16.5	17	19	19	20
Saturated unit weight	γ_{sat}	kN/m^3	16.5	17	19	19	20
Secant stiffness (shear hardening)	E^{ref}_{50}	kN/m^2	10,000	25,000	60,300	25,300	30,000
Tangent oedometer stiffness (compression hardening)	E^{ref}_{oed}	kN/m^2	12,300	21,000	41,600	21,000	38,000
Unloading-reloading stiffness	E^{ref}_{ur}	kN/m^2	30,000	60,000	140,000	60,000	140,000
Power for stress dependent stiffness (hyperbolic model)	m	–	1	1	1	1	1
Reference stress (hyperbolic model)	P_{ref}	kN/m^2	100	100	100	100	100
Cohesion (perfect plasticity limit)	c'	kN/m^2	5	15	10	15	15
Friction angle (perfect plasticity limit)	ϕ'	°	15	28	35	28	28

Table 3 Calibrated parameters of structural elements applied in numerical analysis

Parameter	Symbol	Unit	Pile	Anchor (Grouted part)
Young's modulus in axial direction	E	kPa	15×10^6	14.8×10^6
Unit weight	γ	kN/m^3	24	20
Moment of inertia against bending	I	m^4	4.27×10^{-3}	0.01×10^{-3}
Cross section area	A	m^2	0.32	0.01

Table 4 Calibrated parameters of anchor element (ungrouted part) applied in numerical analysis

Parameter	Symbol	Unit	Anchor (ungrouted part)
Normal stiffness	EA	kN	171.6×10^3
Maximum tension force	$F_{max,tens}$	kN	930
Maximum compression force	$F_{max,comp}$	kN	200

Figures 5 and 6 show the selected excavation section to be modeled (the northern wall of the excavation area) and the geometry of the PLAXIS model. The model included more than 180,000 soil elements, 267,000 nodes and more than 800 structure elements (embedded piles, node-to-node anchors, beams and plates) as shown in Fig. 7.

The boundary condition of the 3D model is normal at the sides, i.e. the horizontal movement is fixed and the vertical movement is free; the bottom surface of the model is totally fixed and the top surfaces are free to move in all directions. To avoid any unwanted boundary effect on the results, the bottom boundary was extended to the depth of 70 m, and the sides of the model was extended away far enough, as shown in Fig. 6.

The traffic loading was simulated by a uniform surcharge of 12 kPa. The building structure adjacent to the excavation area was modeled by a filling material with proper unit weight to provide 300 kPa total vertical stress beneath the building.

At the site, one 15 m span of the soil was excavated 2 meters deep, and then the adjacent 15 m span was left unexcavated (alternate-span excavation). To simulate this excavation procedure in numerical analysis, the geometry of the model of the selected section was discretized in 120 soil blocks with 15 × 15 × 2 m dimensions. In a staged construction mode of calculation, first the soil layering and surroundings surcharges were activated, and then the above mentioned blocks were deactivated one by one until the excavation was modeled thoroughly. At each stage, numerous anchor elements located at the previously excavated layers were activated and pre-stressed to 800 kN. The sequences of excavation in the model was planned to be closet possible to the real excavation stages at the site. A great amount of time, energy, patience and powerful computing hardware was required for such a comprehensive 3D modeling.

Fig. 5 The Northern wall of the excavation preferred for modeling in this study

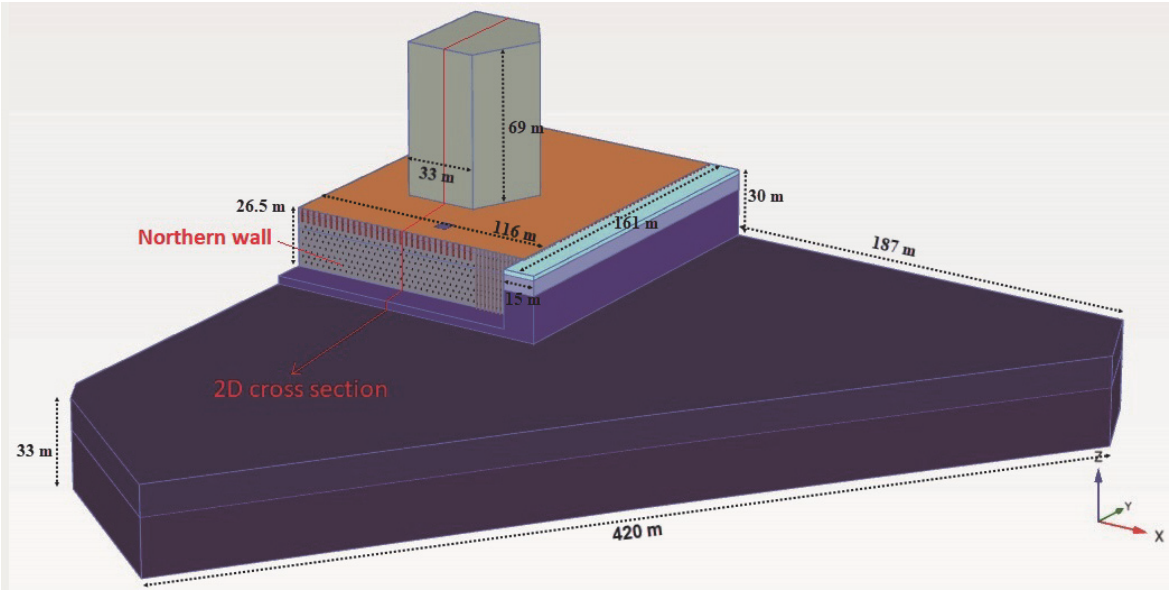

Fig. 6 The geometry of the PLAXIS 3D model of the Northern wall (cross section of the subsequent 2D models is also defined in this figure)

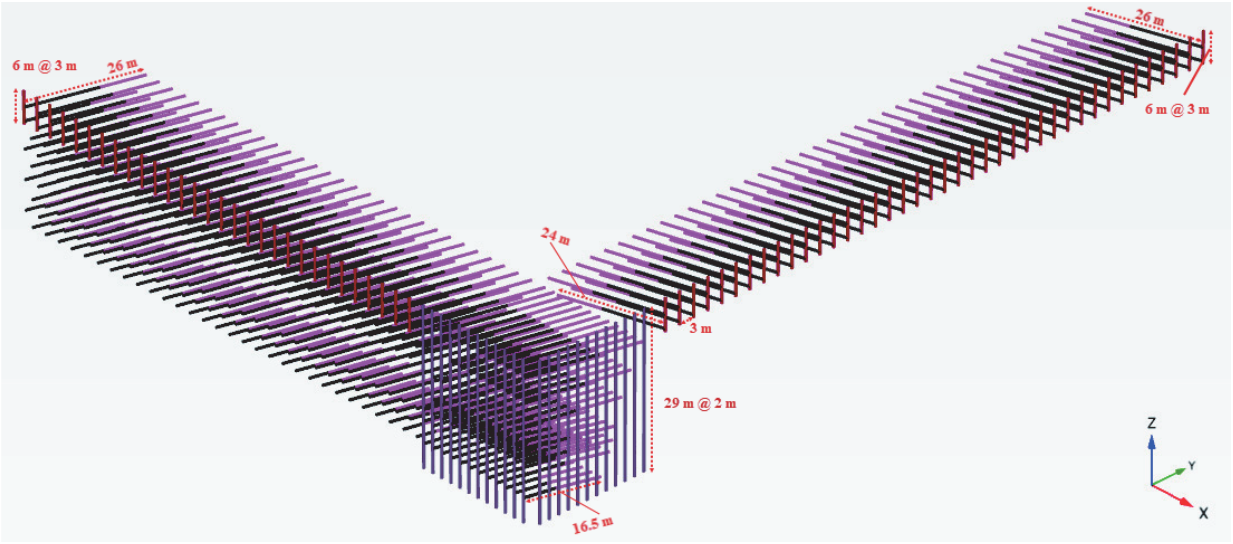

Fig. 7 Structures modelled by PLAXIS 3D including soldier piles and pre-stressed anchors

The main goal of this 3D modelling was to calculate the deformations caused by excavating from 24 m to 26.5 m of depth. Figures 8 and 9 respectively show the horizontal (Y direction) and vertical (Z direction) deformations caused by excavating the first soil block at the western corner. Figures 10 and 11 show the same results after removing all soil blocks and finalizing the excavation.

Figure 12 shows the possible local and total slip surfaces before and after the final excavation stage. The Safety Factor (S. F.) for the final stage is less than one. This factor addresses the local failure possibility at the zone which experiences the most amount of horizontal deformation. In addition to this instability, by the end of the excavation nearly 10 mm of horizontal and 6 mm of vertical deformation was expected to occur in the vicinity of the adjacent tower (as shown in Fig. 10 and Fig. 11). To avoid such risks, strengthening the excavation support was necessary.

Although the PLAXIS 3D was run on a powerful computer (500 GB SSD Hard disk, core i7 @2.2 GHz CPU and 16 GB RAM), a lot of time was consumed to create and calculate only one 3D model (3 weeks for one model). Due to the numerous strengthening scenarios which were to be tried numerically, it was not economic to continue 3D modeling. However, the problem with 2D modeling was the lack of capabilities to simulate the alternate-span excavation method. The innovation of this study was to find a way to simulate the alternate-span excavation method in the 2D models by adding a "virtual berm" at the toe of the excavated wall. The berm is virtual because it was only created in numerical models and did not exist in reality. The berm properties were calibrated with the help of the 3D models: the soil model was the same with the soil layer at the excavation final depth and the berm height was 10% of the excavation final depth (*i.e.,* 2.5 m in 26.5 m). The comparison of the 2D and 3D results show that this virtual berm in 2D models could play the role of the alternate removal of soil blocks in the 3D models.

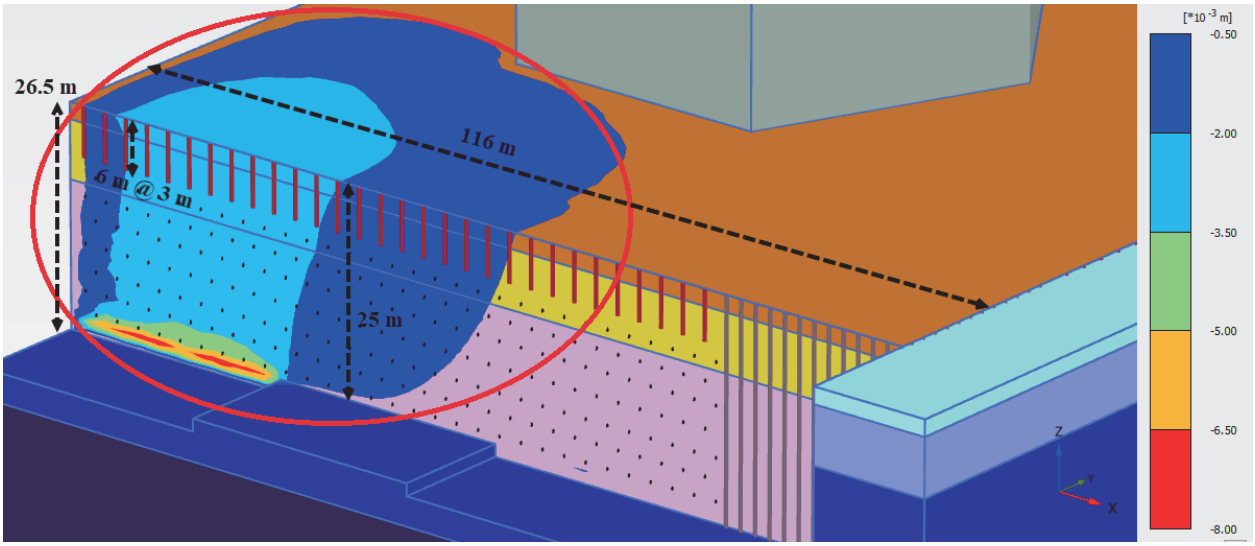

Fig. 8 Horizontal deformation (Y direction) caused by excavating the first soil block at the western corner of the northern wall

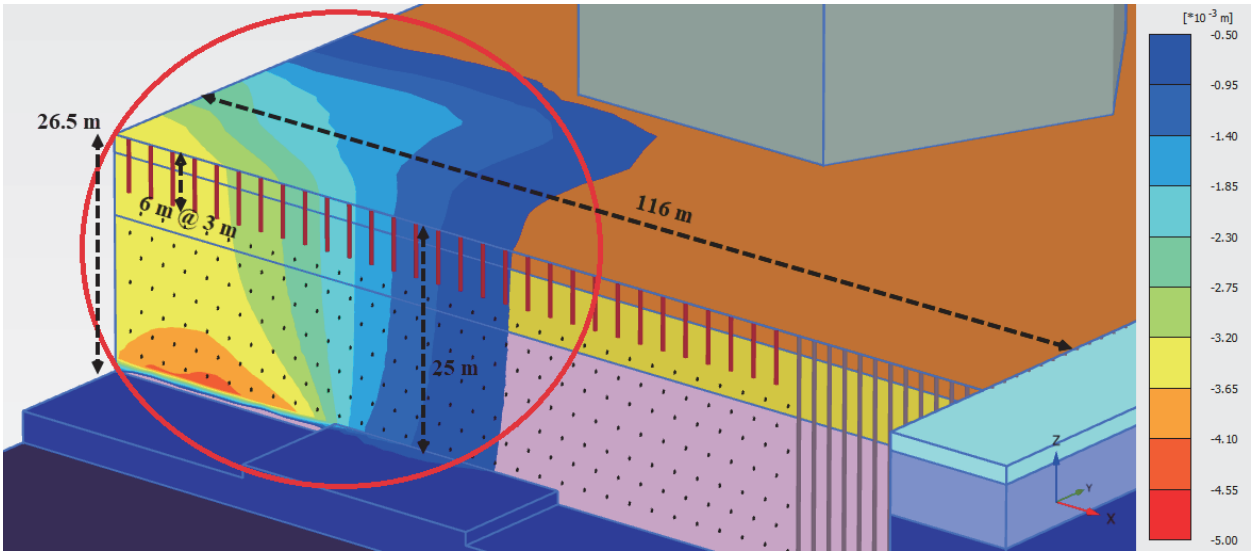

Fig. 9 Vertical deformation (Z direction) caused by excavating the first soil block at the western corner of the northern wall

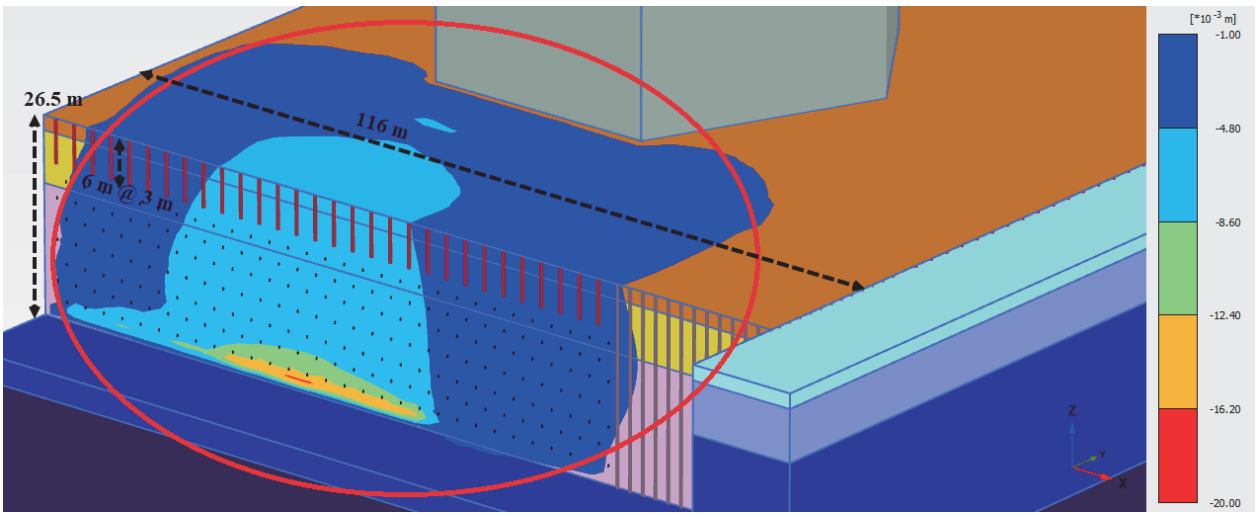

Fig. 10 Horizontal deformation (Y direction) caused by excavating the last block at the middle of the northern wall

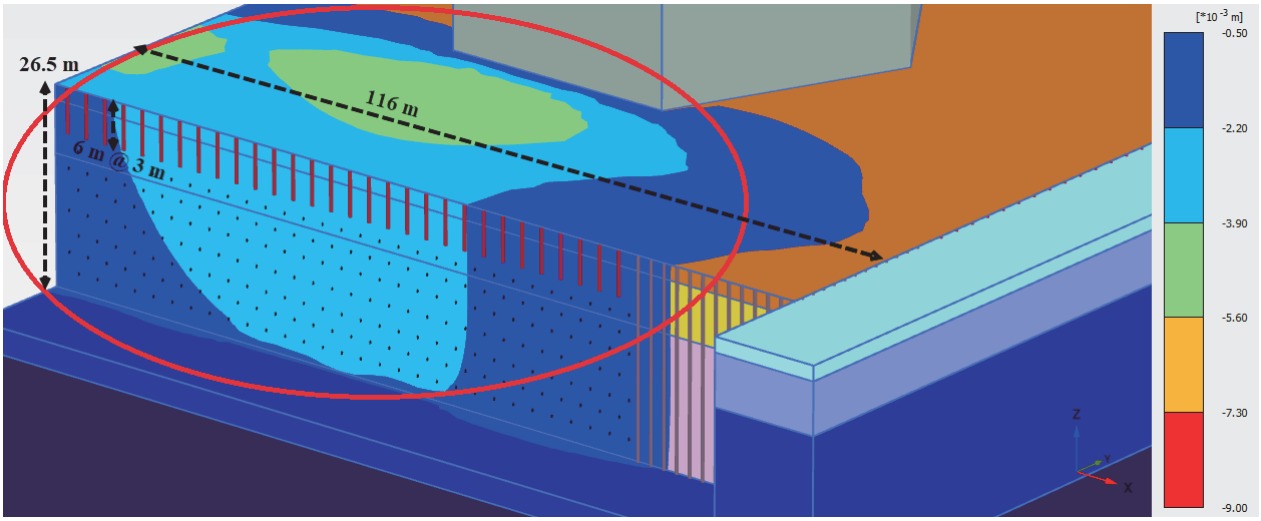

Fig. 11 Vertical deformation (Z direction) caused by excavating the last block at the middle of the northern wall

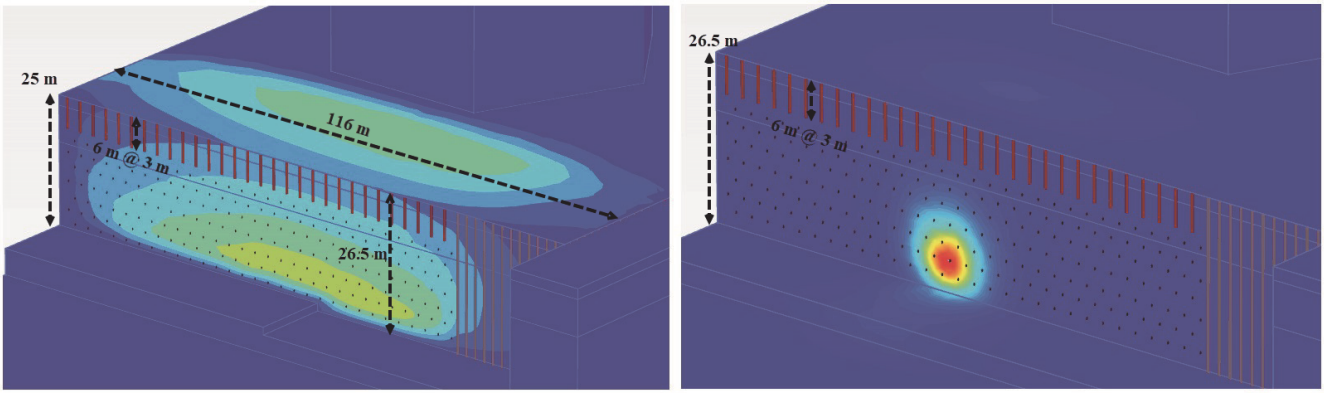

(a) Before the final stage of excavation: S.F. = 1.57 (b) After the final stage of excavation: S.F. = 0.1

Fig. 12 Excavation stability analysis by the strength reduction technique

3.2 2D Calculations

For 2D plane strain analysis, PLAXIS 2D 2016 was used (PLAXIS 2D 2016). In 2D models, both sides were free to move vertically but fixed horizontally, while the bottom line was totally fixed. Similar to 3D models, boundaries were extended away far enough to avoid unwanted effects on the results. Figure 13 shows deformations of the wall due to the final stage of excavation (from 24 m to 26.5 m). The comparison of the 2D and 3D results (Fig. 10 and Fig. 13) show a considerable difference; taking into account the similar geometry and material model used in both calculations, this difference clarifies the importance of modeling the alternate-span excavation procedure.

Figure 14 shows the idea of the virtual berm which helped modeling alternate excavation in a 2D model. As evident in this figure, the magnitude of horizontal deformations after activating the last anchor, is close to the 3D results (Fig. 10), though there are some differences in the distribution pattern of deformation contours in Fig. 10 and Fig. 14. The virtual berm simulates the span of soil which remains unexcavated in an alternate-span excavation (Fig. 4 and Fig. 8).

Figure 15 shows the possible slip surface of the model with the virtual berm; the slip surfaces geometry and Safety Factor is close to those of the 3D model shown in Fig. 12(a). To improve the initial design, several scenarios were modeled. The base model in these calculations benefited from the virtual berm idea. The scenarios included different distributions of anchors in both directions and different lengths of bonding and pre-stressing magnitudes. Figure 16 shows the preferred scenario for the optimized design, which included 3 extra rows of anchors in addition to the previous ones (marked with circles in Fig. 16). The same as previous figures, this figure shows the horizontal deformation after excavating form 24 m to 26.5 m (the final excavation phase). Although the maximum phase deformation is not much different from the non-reinforced model shown in Fig. 14, the distribution is different: In the optimized design, the zone of maximum deformation moved to a limited area in the surficial layers.

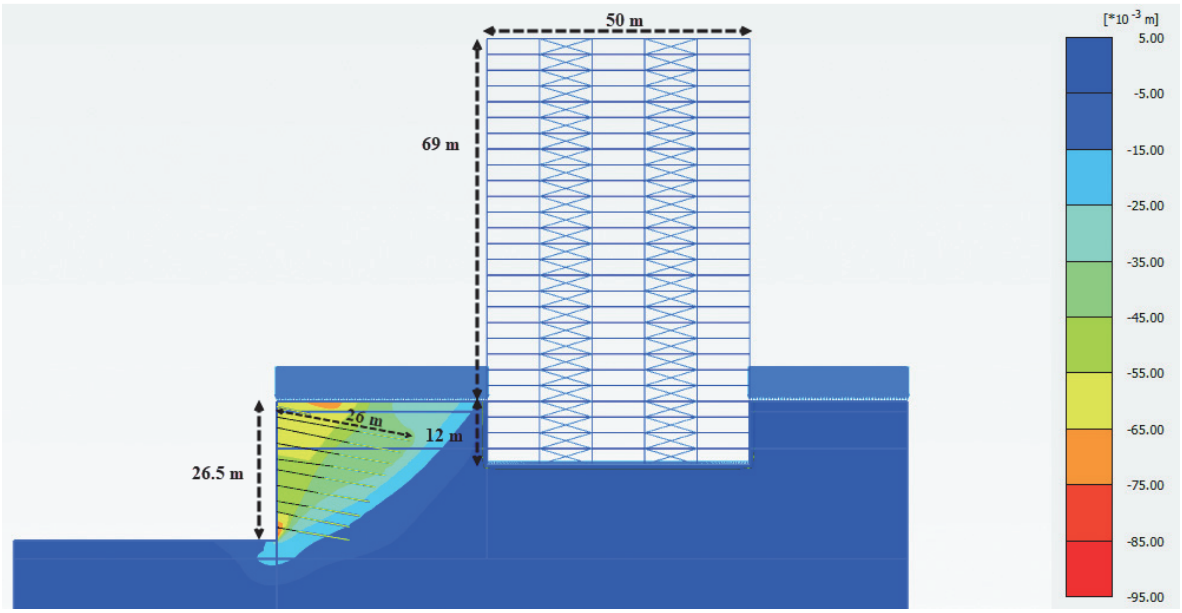

Fig. 13 Horizontal deformation after the last phase of excavation

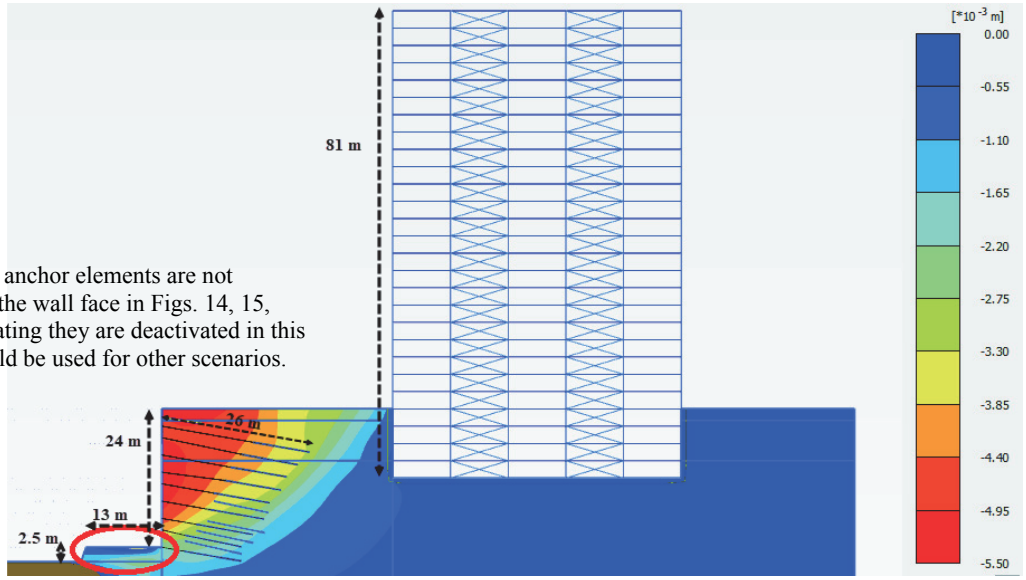

Remarks: Some anchor elements are not connected to the wall face in Figs. 14, 15, and 16, indicating they are deactivated in this case and would be used for other scenarios.

Fig. 14 Horizontal deformation after the last phase of excavation – with the virtual berm

4. CONSTRUCTION AND MONITORING

With the optimized design, the excavation continued with the alternate-spans technique and added precise monitoring. Although the analyses were conducted assuming 15 m spans of excavation, it was recommended to decrease the span lengths to 5 meters at the field in some areas. To conduct precise monitoring of the deformations, 6 inclinometers were installed at northern walls of the site as shown in Fig. 17 (Khak Energy Pars 2017). Inclinometers numbered 6 and 7 which are marked in Fig. 17, were located on the northern wall of the excavation at site A1, which was modelled in the present study.

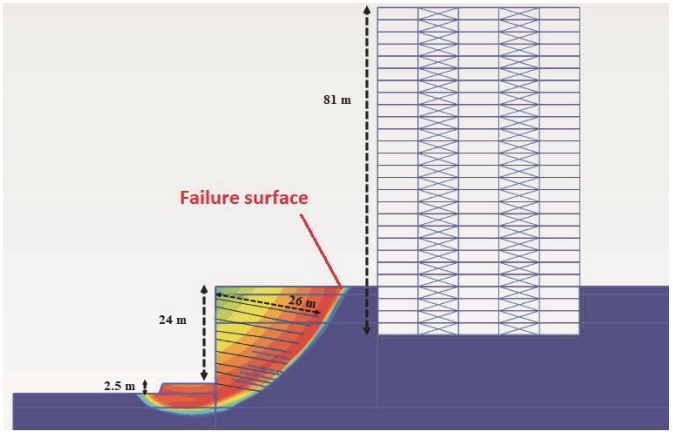

Fig. 15 Excavation stability analysis by the strength reduction technique: S.F. = 1.47

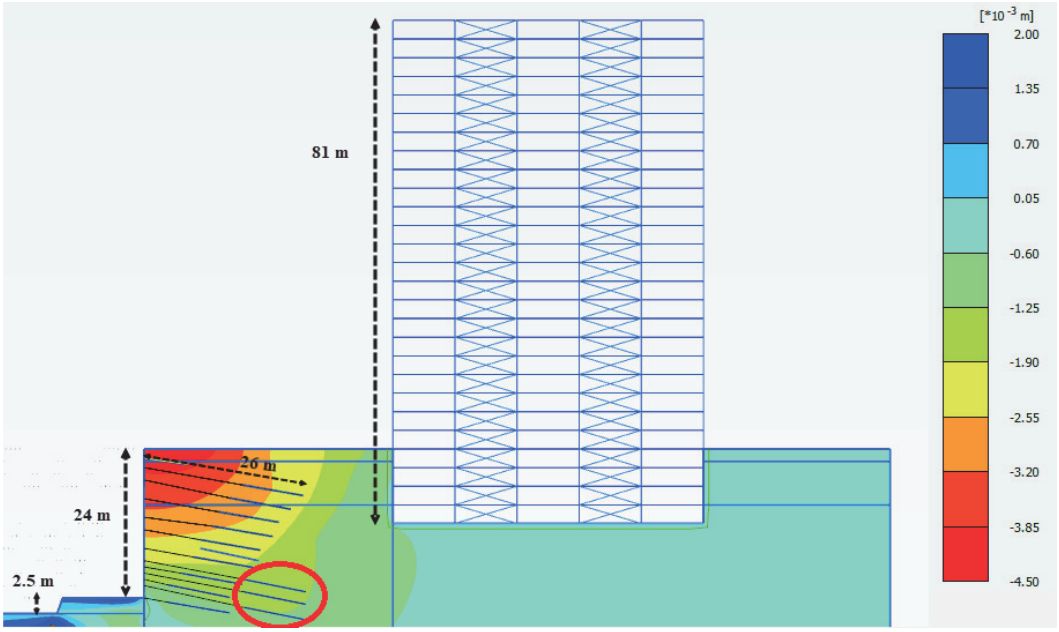

Fig. 16 Horizontal deformation after the last phase of excavation – the optimized design

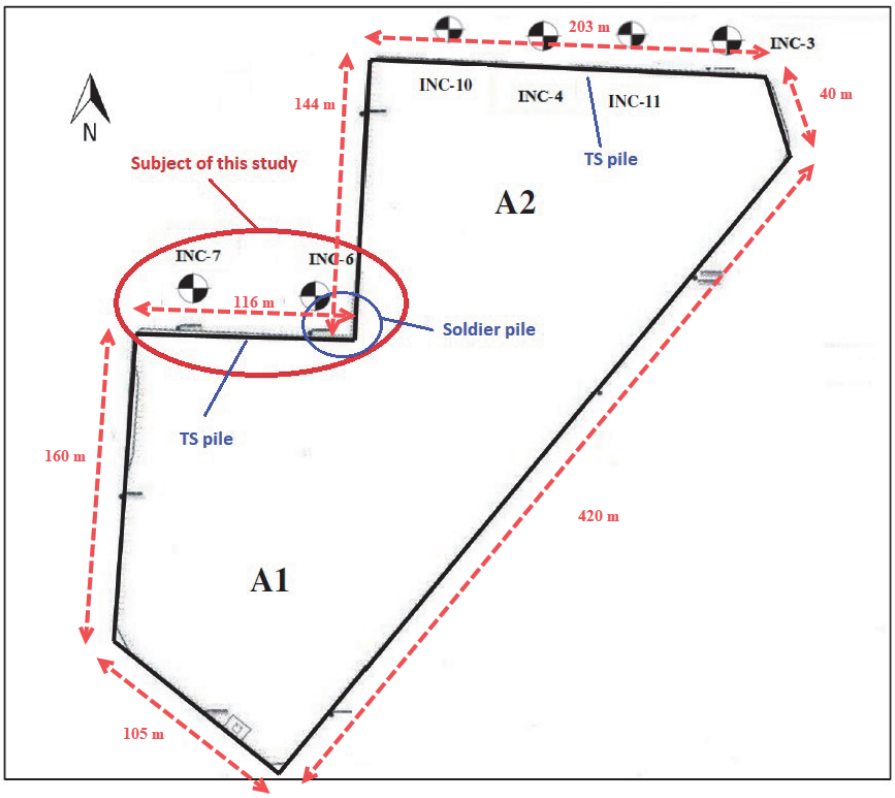

Fig. 17 The inclinometer locations along Northern walls

5. RESULTS AND DISCUSSION

5.1 Comparison between Measured and Predicted Results

Figures 18 and 19 show inclinometers readings during and after the completion of the northern wall excavation at site A1. End of excavation is defined in each case.

The pattern and magnitude of deformations derived from inclinometer No. 7 coincide satisfactorily with the optimized design calculations, as shown in Fig. 20. Subsequent deformations measured by the inclinometer seem to relate to the creep of the anchors. The optimized design was completely satisfactory.

Inclinometer No.6 is expected to show limited deformation, because it is located among soldier piles extended beneath the bottom of the excavation (270° corner in Fig. 7).

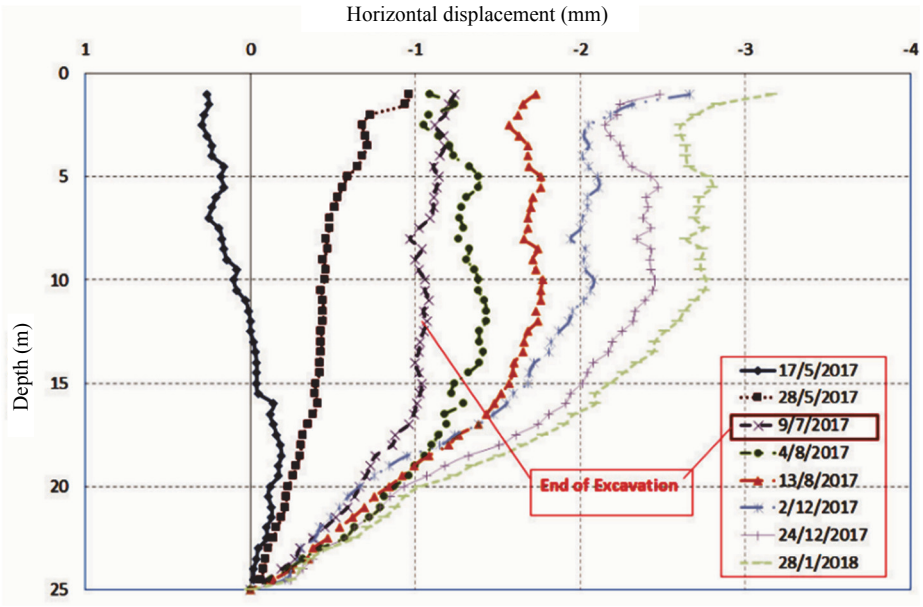

Fig. 18 Readings of inclinometer No. 6

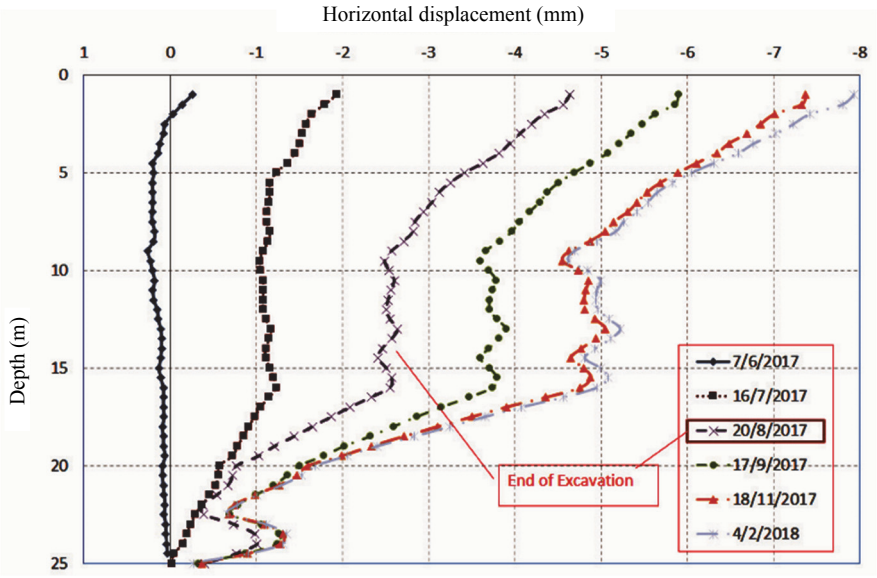

Fig. 19 Readings of inclinometer No. 7

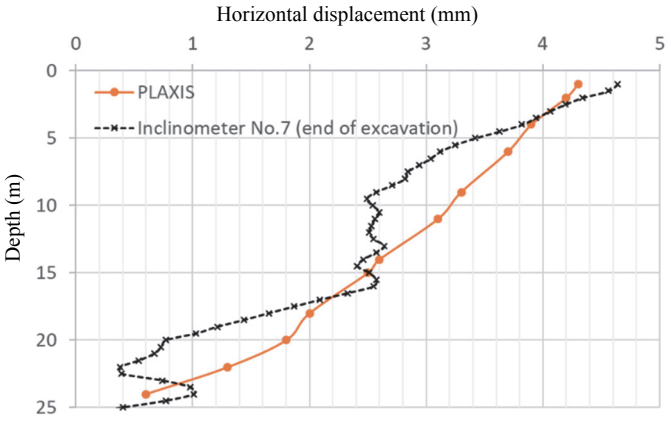

Fig. 20 Comparison of inclinometer No. 7 readings with PLAXIS calculations

5.2 Evaluation of the TS Pile Behavior

The main disadvantage of the initial design in the studied excavation was the lack of vertical support of the retaining structure (shotcrete and anchors), which lead to disturbing cracks in the neighboring areas. The vertical support is usually provided by the embedded depth of a soldier pile, installed from the surface down to a depth beneath the excavation bottom. TS piles do not provide such a support and should not replace the soldier piles.

In the present study, the important role of the soldier pile was clearly observed by comparing the monitoring measures near soldier piles (inclinometer 6 in Fig. 17) with those only containing TS piles (inclinometer 7 in Fig. 17), as shown in Fig. 21.

Figure 21 shows maximum measurements of the inclinometers shown in Fig. 17, from the installation stage up to the time of writing this paper; the maximum readings mostly belong to the locations near the surface. Inclinometers 3, 4, 10, and 11 are installed among TS piles at north of A2 site (Fig. 17) and inclinometers 6 and 7 are located at north of A1 site, among soldier

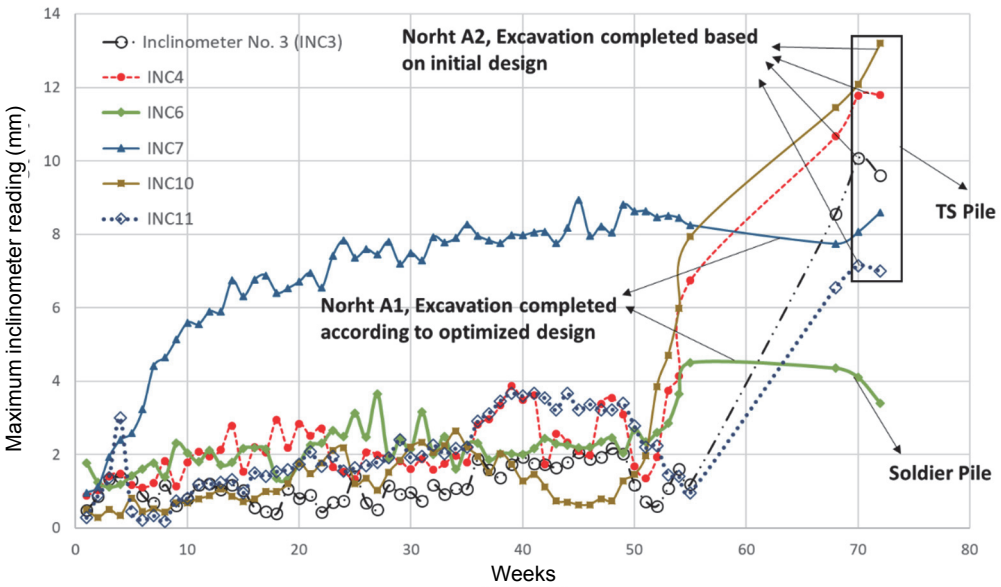

Fig. 21 Maximum readings of inclinometers at northern walls, from installation stage up to end of excavation

piles of the 270° corner and TS piles of the remaining of the wall, respectively (Fig. 7 and Fig. 17). The excavation proceeded wall by wall, which may be detected in Fig. 21 as the sudden rise of the readings. Comparison of inclinometers 6 and 7 shows the difference of TS pile and soldier pile behavior. Although the excavation near these two inclinometers was completed simultaneously, it is however worth noting that the remaining soil to be excavated after inclinometers installation, was few meters higher next to inclinometer 7; this may explain some of the differences between readings of inclinometer 6 and 7. The lack of cracks near soldier piles compared with propagated cracks near TS piles was another evidence: The rigidity caused by the soldier piles reduced the deformation of the surrounding area compared with the flexibility of TS piles and consequently relatively larger deformations, though the retaining structure at north of site A1 was optimized by the authors, as stated in previous sections of this paper.

The importance of the optimization stated in this paper is obvious while comparing inclinometer 7 readings with inclinometers 3, 4, 10, and 11 readings in Fig. 21. The deformations of inclinometers at north of site A2 has exceeded those at north of A1. This is because the optimization of the initial design was not followed in excavation of north of A2 site.

6. CONCLUSIONS

(1) Although TS piles increase local stiffness for the area behind them, they do not provide vertical support required for a stable retaining structure. They should not be replaced with soldier piles in the Berlin method of excavation.

(2) Numerical modeling is a practical and precise tool to design excavations, if utilized correctly. Suitable constitutive models must be employed with the most possible similarity to the real soil behavior. On the other hand, sufficient preliminary geotechnical investigation is required to calibrate constitutive models as precise as possible.

(3) In addition to an accurate geometry and soil behavior modeling, the calculation phases of a numerical analysis must also resemble the actual construction sequences at the site.

(4) To design an optimal retaining structure for an excavation, sometimes it is necessary to try different scenarios. However, it is not practical to conduct many 3D calculations. On the other hand, some construction techniques cannot directly be modelled in a 2D code, like the alternate-span excavation. In the present case study, noteworthy difference of results was observed in the 3D calculations (while considering alternate-span technique) and the routine 2D calculations (where the alternate-span excavation technique had not been considered in the model).

(5) To conduct accurate and economic analyses, in this study a preliminary detailed 3D modelling was first conducted; then a 2D model containing a virtual supporting berm was evaluated according to the 3D results. The virtual berm in the 2D modeling simulated the alternate-span excavation in the 3D modeling. The optimized design was selected among different scenarios which were executed by plenty 2D analyses on the basic model with the virtual berm.

(6) The deformation monitoring which began after the design optimization at the second stage of excavations, showed magnitudes satisfactorily similar to the calculation results. This closeness of the monitoring and analyses results confirms the strength of the numerical modeling guidelines followed in this case study.

(7) Comparing the two adjacent excavation faces with similar soil layers, but different retaining structures, showed the unacceptable behavior of the TS piles: The northern wall at site A1 strengthened with TS piles and 9 rows of anchors, was not as rigid as its corner, retained by soldier piles and only 7 rows of anchors. While the latter was finished with limited deformation, the former caused crack propagation in neighboring areas.

(8) The present study discourages engineers and contractors from using TS piles instead of soldier piles.

ACKNOWLEDGMENTS

This study was supported by the client, consultant and contractor of the Jahan Mall project via KDHT Corporation. The authors gratefully acknowledge the support of KDHT and also thank Mr. Niknam and Kareno Technologies Corporation for facilitating the access to PLAXIS 3D and 2D licenses. The International Institute of Earthquake Engineering and Seismology is also highly acknowledged for the valuable help and support via research projects No. 711 and No. 675.

NOMENCLATURE

A	Cross section area (m^2)
c'	Cohesion (perfect plasticity limit) (kN/m^2)
C_c	Compression index
C_s	Swelling (recompression) index
EA	Normal stiffness (kN)
EI	Flexural rigidity ($kN \cdot m^2/m$)
E	Young's modulus in axial direction (loading) (kN/m^2)
E_p	Young's modulus measured by pressuremeter test (kN/m^2)
E_s	Young's modulus measured by SPT N value or Triaxial test (kN/m^2)
E_r	Young's modulus in axial direction (unloading-reloading) (kN/m^2)
E^{ref}_{50}	Secant modulus (shear hardening) (kN/m^2)
E^{ref}_{oed}	Tangent oedometer modulus (compression hardening) (kN/m^2)
E^{ref}_{ur}	Unloading-reloading modulus (kN/m^2)
$F_{max,tens}$	Maximum tension force (kN)
$F_{max,comp}$	Maximum compression force (kN)
ϕ'	Friction angle (perfect plasticity limit) (°)
γ	Unit weight (kN/m^3)
γ_{unsat}	Unsaturated unit weight (kN/m^3)
γ_d	Dry unit weight (kN/m^3)
γ_{sat}	Saturated unit weight (kN/m^3)
I	Moment of inertia against bending (m^4)
m	Power for stress dependent stiffness (hyperbolic model)
ν	Poisson's ratio
P_c	Pre-consolidation pressure (kN/m^2)
P_{ref}	Reference stress (hyperbolic model) (kN/m^2)

REFERENCES

Brinkgreve, R.B.J., Swolfs, W.M., and Engin, E. (2016). *Plaxis, Finite Element Code for Soil and Rock Analysis*, *User's Manual*, Version 2016, Plaxis bv., the Netherlands.

Jahad Azma Co. (2015). *Geotechnical Investigation Report*, Jahan Mall Project.

Khak Energy Pars Co. (2017). *Monitoring Report*, Jahan Mall Project.

Plaxis 3D (2016). *3D Finite Element Code*, Version 2016. Plaxisbv, Delft, the Netherlands.

Plaxis 2D (2016), *2D Finite Element Code*, Version 2016. Plaxisbv, Delft, the Netherlands.

Puller, M. (2003). *Deep Excavations: A Practical Manual*. Thomas Telford.

Sabatini, P.J., Pass, D.G., and Bachus, R.C. (1999). *Geotechnical Engineering Circular No. 4: Ground Anchors and Anchored Systems*, No. FHWA-IF-99-015.

Schanz, T., Vermeer, P.A., and Bonnier, P.G. (1999). "The hardening-soil model: Formulation and verification." Brinkgreve, R.B.J., Ed., *Beyond 2000 in Computational Geotechnics*, Balkema, Rotterdam, 281-290.